Supplementary Information

Microenvironment-feedback regulated hydrogels as living wound healing materials

Yibo Cheng†, Yanwen Wang†, Yunyi Wang†, Poh-Ching Tan*, Shiyun Yu, Chi Li, Zi-Yuan Li, Qing-Feng Li, Shuang-Bai Zhou*, Chen Wang*, Junji Zhang*, He Tian

Y. Cheng, S. Yu, Z. Li, J. Zhang, H. Tian

Institute of Fine Chemicals, School of Chemistry and Molecular Engineering, East China University of Science and Technology, Shanghai 200237, China

Y. Cheng, Y. Wang, C. Li, C. Wang

School of Chemistry and Molecular Engineering, East China Normal University, Shanghai 200241, China

Y. Wang, P. Tan, Q. Li, S. Zhou

Department of Plastic and Reconstructive Surgery, Shanghai Ninth People's Hospital, Shanghai Jiao Tong University School of Medicine, Shanghai, China

Corresponding authors: zhangjunji@ecust.edu.cn, cwang@chem.ecnu.edu.cn, bojun_tan@hotmail.com, shuangbaizhou@yahoo.com.

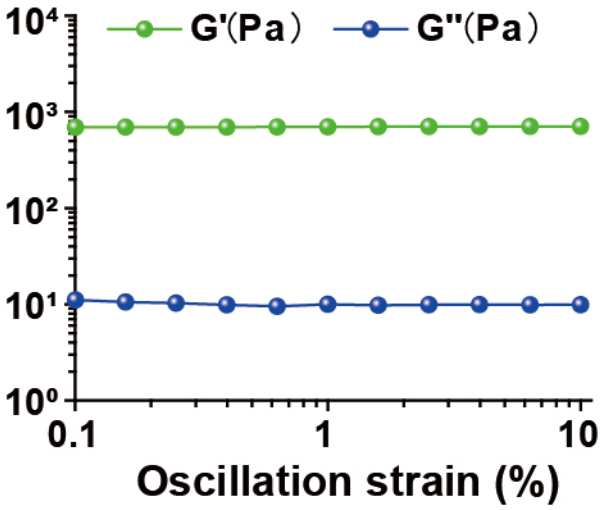

Supplementary Figure 1. Oscillatory amplitude sweeps of OSA-GEL hydrogel at angular frequency of 10 rad/s and strain from 0.1% to 10%. Source data are provided as a Source Data file.

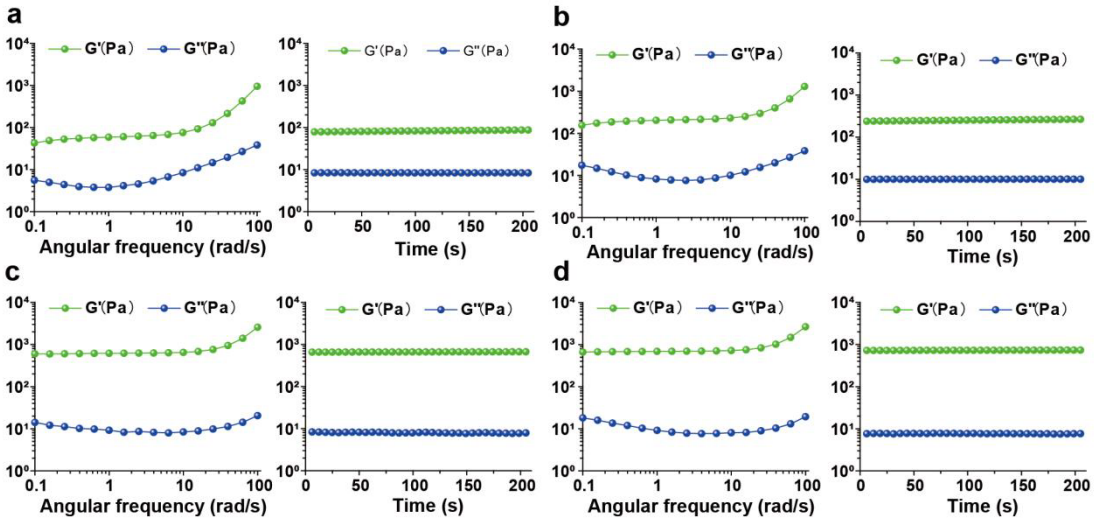

Supplementary Figure 2. Rheological data of gels prepared with different proportions of OSA:GEL, (a) 2:1; (b) 1:1; (c) 1:2; (d) 1:3. Source data are provided as a Source Data file.

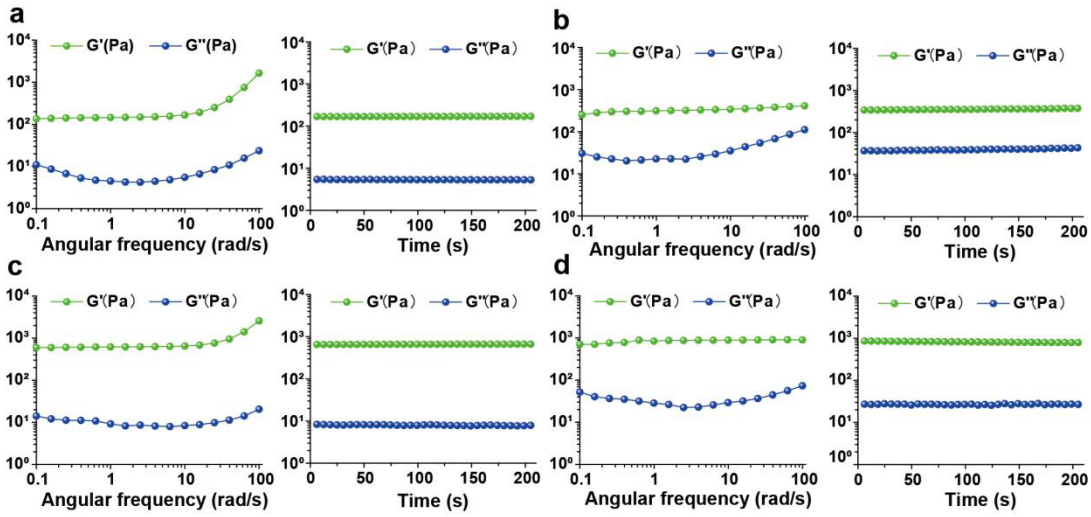

Supplementary Figure 3. Rheological data of gels at different weight concentrations; (a) 10%; (b) 12%; (c) 15%; (d) 18%. Source data are provided as a Source Data file.

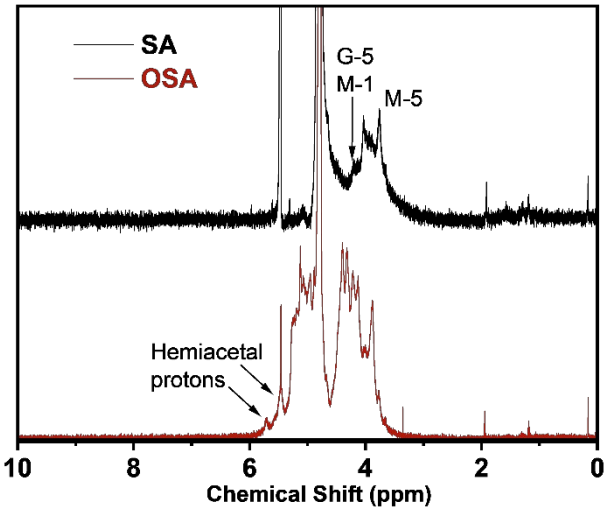

Supplementary Figure 4. ^{1}H NMR spectra of sodium alginate (SA) and oxidized sodium alginate (OSA). Source data are provided as a Source Data file.

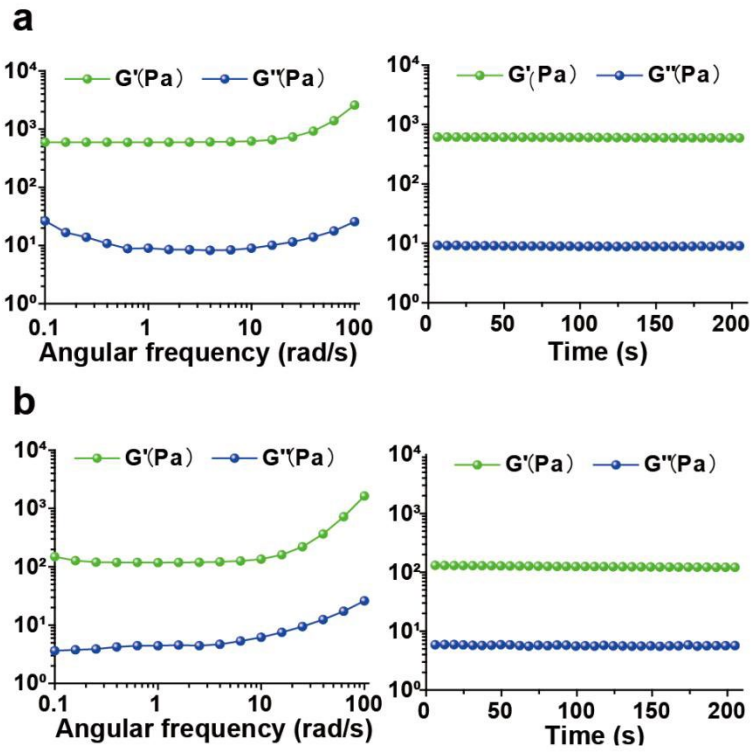

Supplementary Figure 5. Schematics of G' and G'' of gels at different pH as function of frequency and time; (a) pH = 8; (b) pH = 5. Source data are provided as a Source Data file.

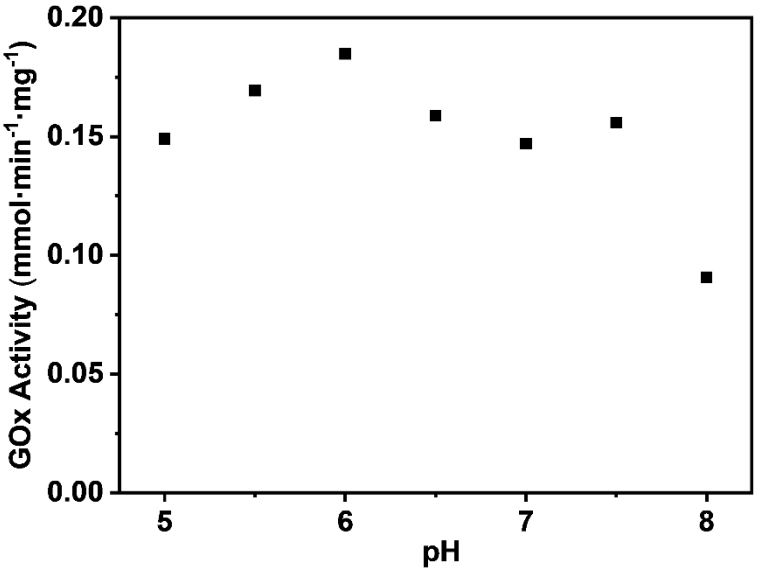

Supplementary Figure 6. GOx activity as a function of pH. Source data are provided as a Source Data file.

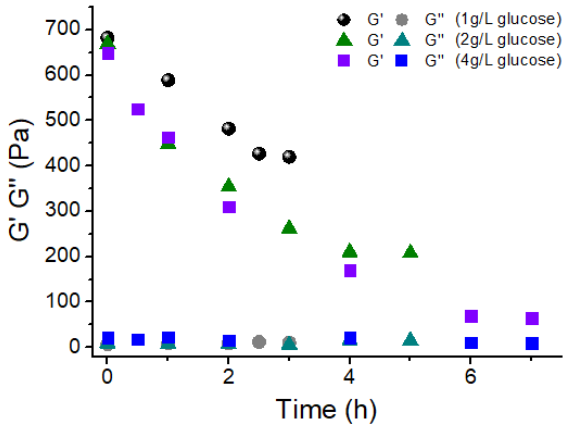

Supplementary Figure 7. Rheological changes of gel dissociation at glucose concentration of 1 g/L, 2 g/L, 4 g/L, respectively. Source data are provided as a Source Data file.

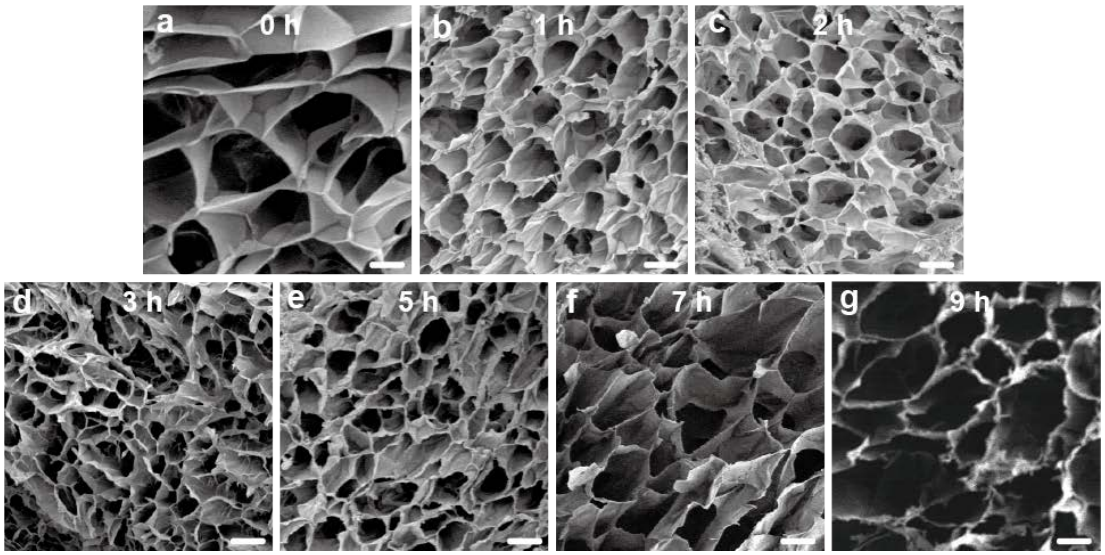

Supplementary Figure 8. SEM images of **OSA-GEL@G** hydrogel at different time (t = 0 min represents the starting point of the second cycle), scale bar is 10 μm.

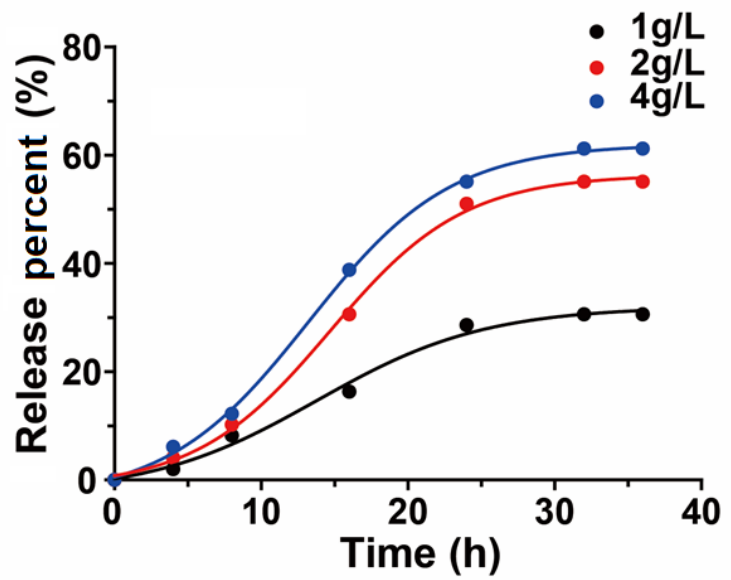

Supplementary Figure 9. The release percent of GOx over time at different glucose concentrations. Source data are provided as a Source Data file.

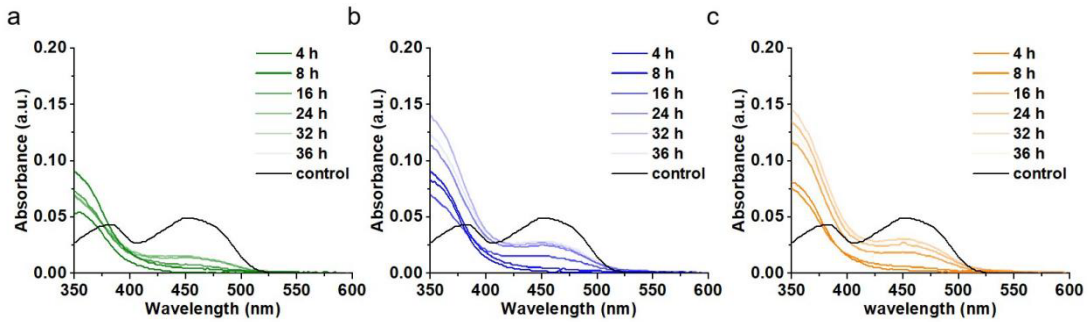

Supplementary Figure 10. UV absorption spectra of released GOx over time at different glucose concentrations; (a) Glucose concentration 1 g/L; (b) Glucose concentration 2 g/L; (c) Glucose concentration 4 g/L. In all experiments, control group is GOx solution (c = 0.5 g/L). Source data are provided as a Source Data file.

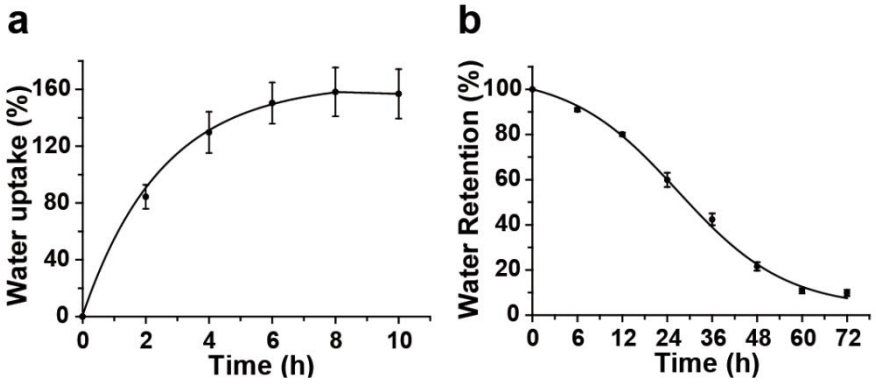

Supplementary Figure 11. Water uptake (a) and retention (b) properties of hydrogels. (n = 3 independent technical samples, Data in are presented as mean values +/- SD. Source data are provided as a Source Data file.

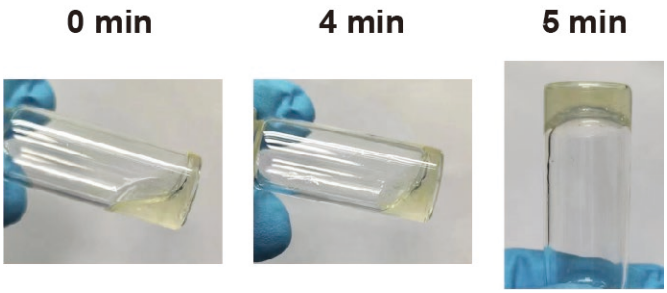

Supplementary Figure 12. The photographs of **OSA-GEL@G** hydrogels in upside-down vial experiments, indicating the rapid gelation process.

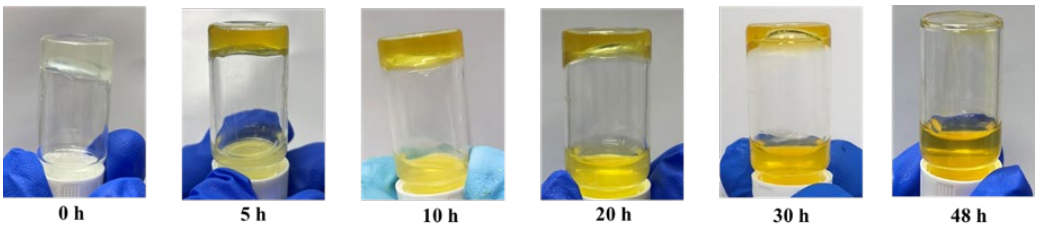

Supplementary Figure 13. Photographs showing the dynamic process of **OSA-GEL@G** hydrogel to the dissociated liquid state, in which [GOx] = 0.1 g/L, [glucose] = 4g/L.

Supplementary Figure 14. Shape adaptability of **OSA-GEL@G** hydrogel.

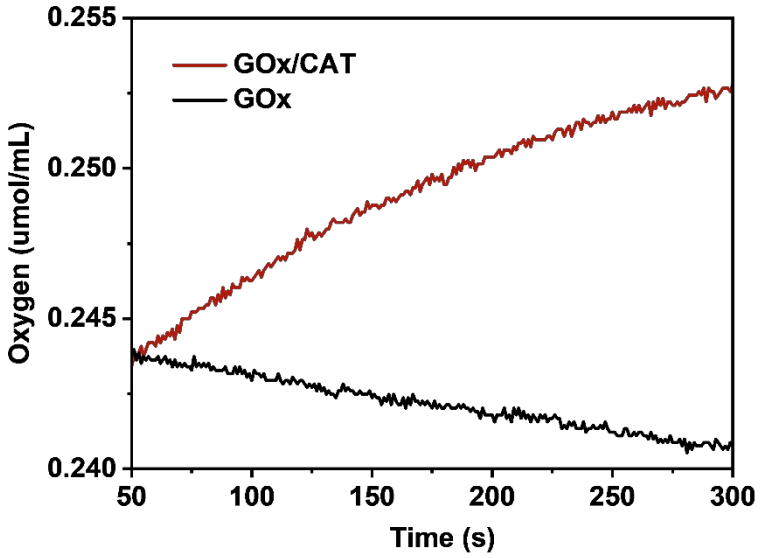

Supplementary Figure 15. Time-dependent oxygen content in the OSA-GEL@GC hydrogel-treated group (red curve) and OSA-GEL@G hydrogel-treated group (black curve), respectively. Source data are provided as a Source Data file.

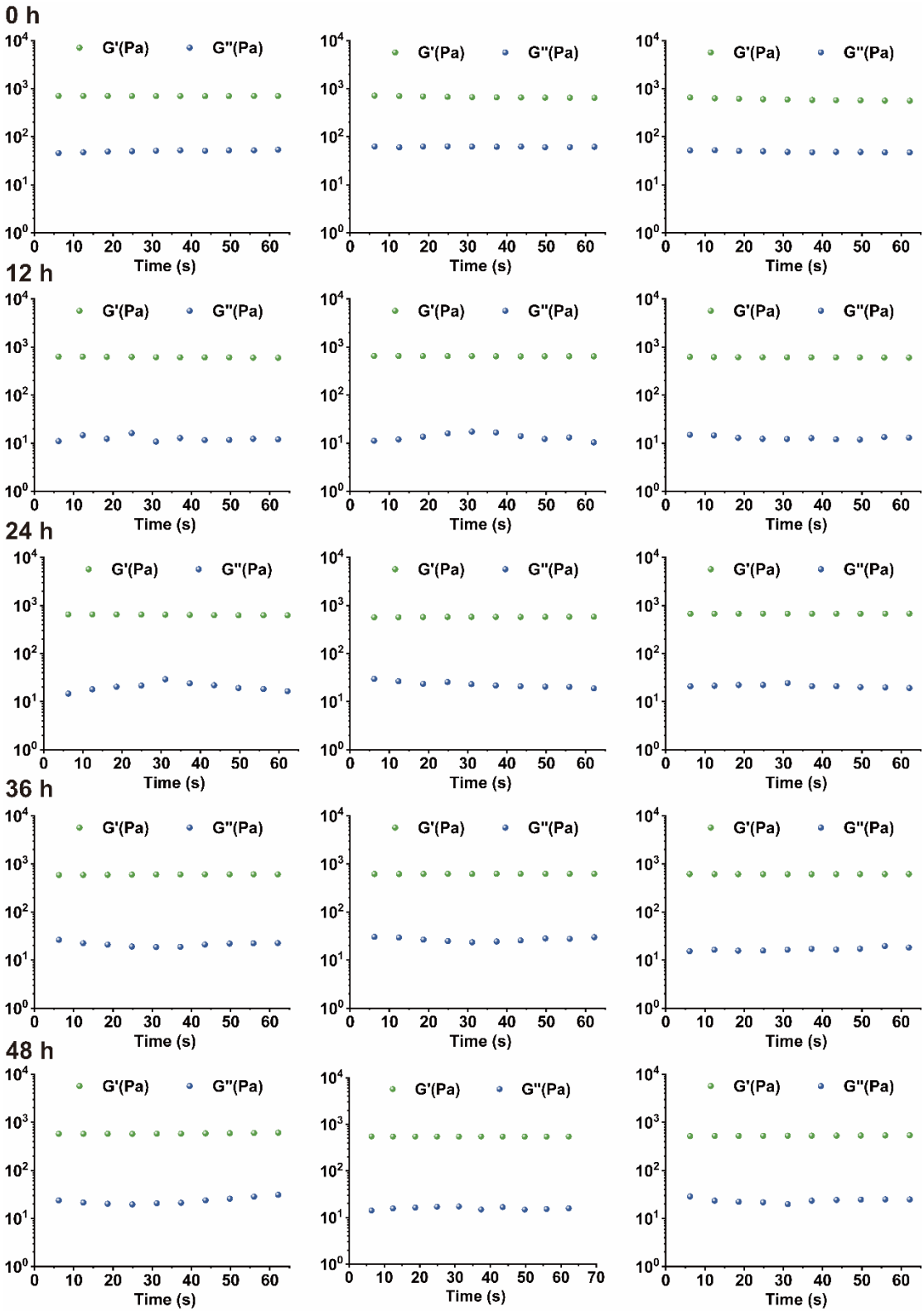

Supplementary Figure 16. Time-dependent rheological data of OSA-GEL on wound bed on different time intervals. Source data are provided as a Source Data file.

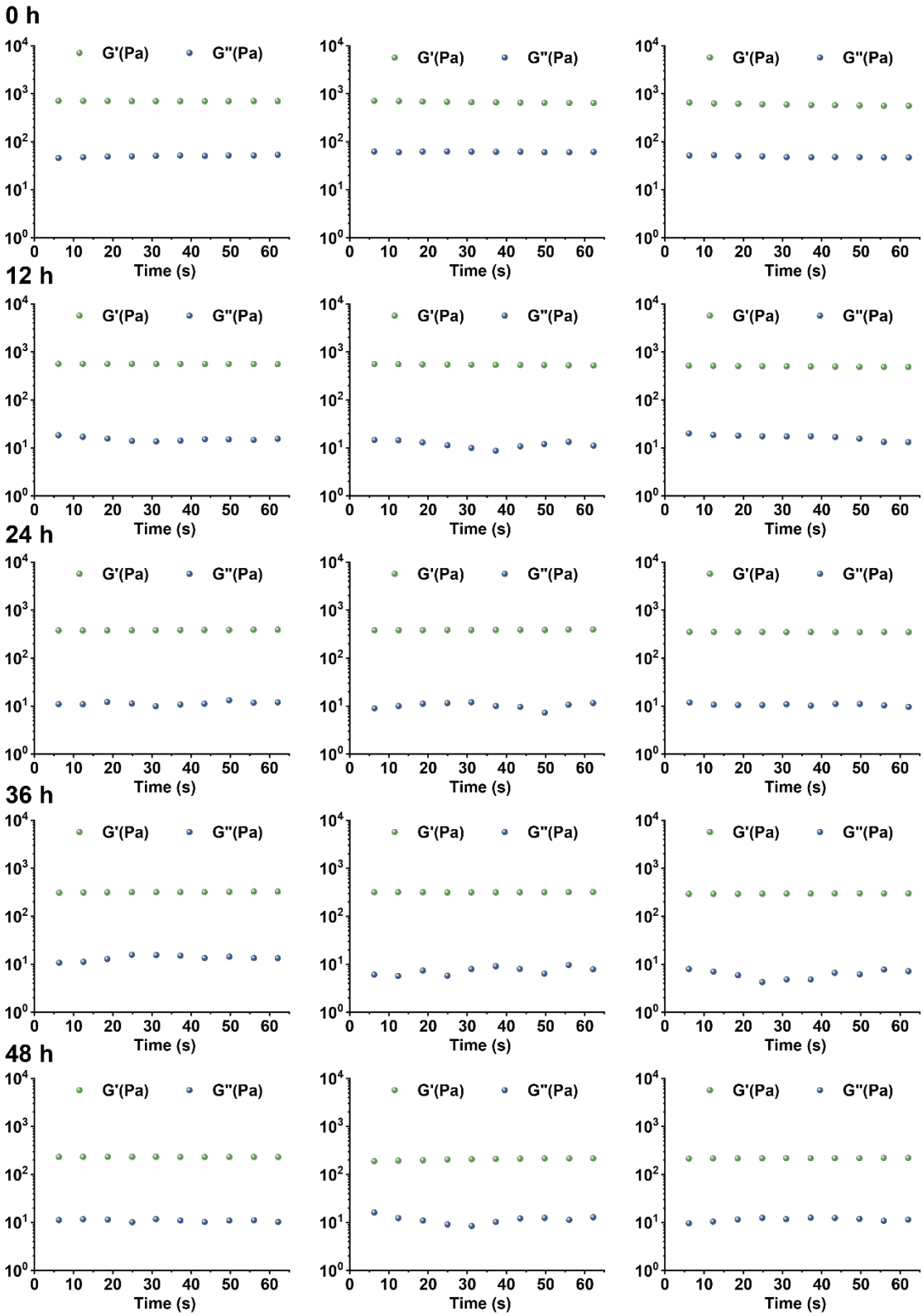

Supplementary Figure 17. Time-dependent rheological data of **OSA-GEL@GC** on wound bed on different time intervals. Source data are provided as a Source Data file.

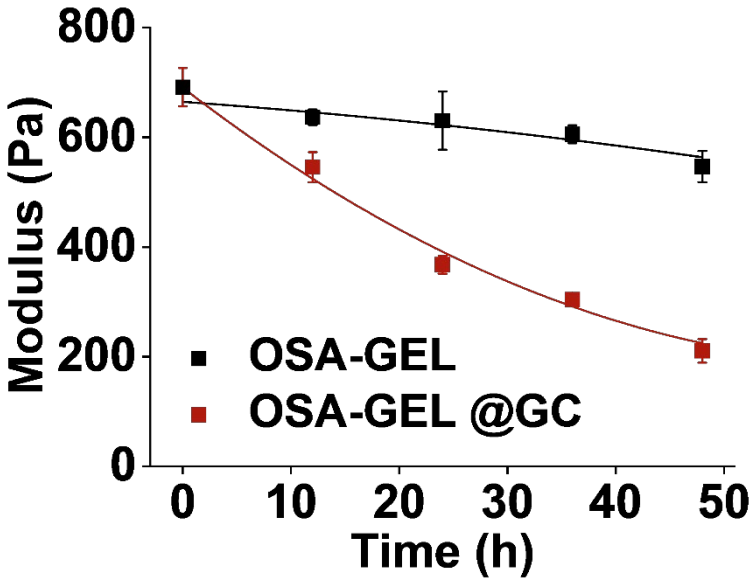

Supplementary Figure 18. Time-dependent gel degradation of hydrogel dressings on diabetic wound bed. Red: OSA-GEL@GC; Black: OSA-GEL. (n = 3 independent samples, Data in are presented as mean values +/- SD. Source data are provided as a Source Data file.

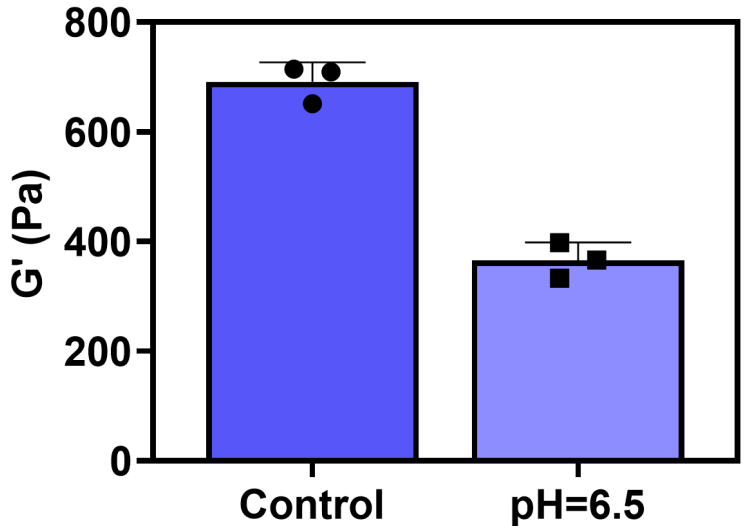

Supplementary Figure 19. Rheological data of **OSA-GEL@GC** under relatively acidic pH of 6.5. (n = 3 independent samples, Data in are presented as mean values +/- SD. Source data are provided as a Source Data file.

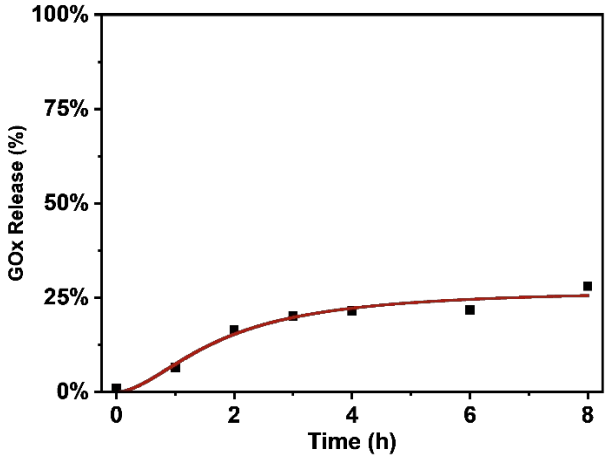

Supplementary Figure 20. Release of GOx from the hydrogel over time under the condition of pH 6.5. Source data are provided as a Source Data file.

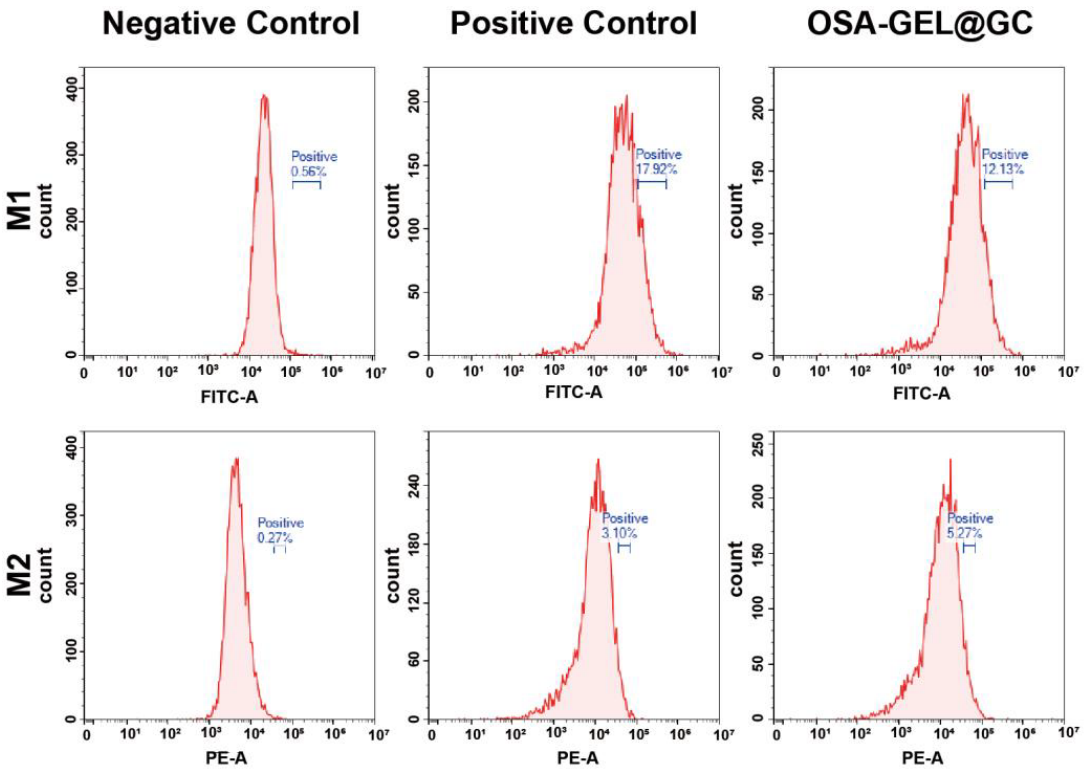

Supplementary Figure 21. Polarization data of induced RAW 264.7 to M1 and M2 phenotypes by flow cytometry. Experiments were repeated three times independently. Source data are provided as a Source Data file.

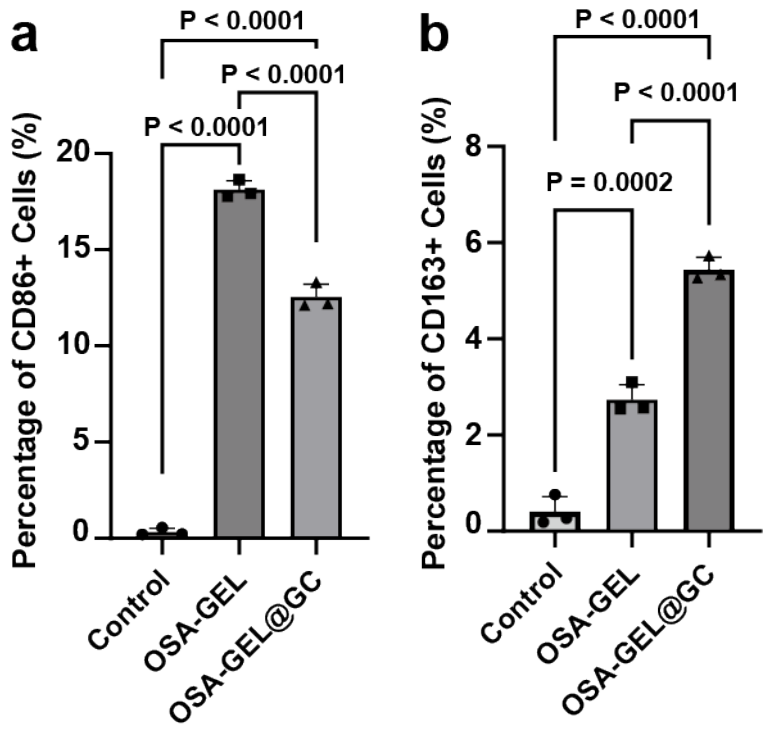

Supplementary Figure 22. Statistical analyses of RAW 264.7 macrophage M1 (CD86+) or M2 (CD163+) polarization: (a) CD86; (b) CD163 (n = 3 independent samples). Data in (a and b) are presented as mean values +/- SD. Data analyzed by one-way analysis of variance with two-sided Tukey's multiple comparisons test (a and b). Source data are provided as a Source Data file.

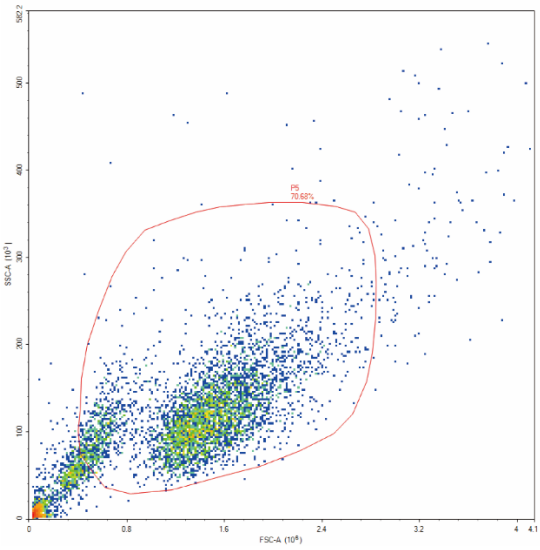

Supplementary Figure 23. Representative gating for data analyzed of M1 polarization in Supplementary Fig. 21.

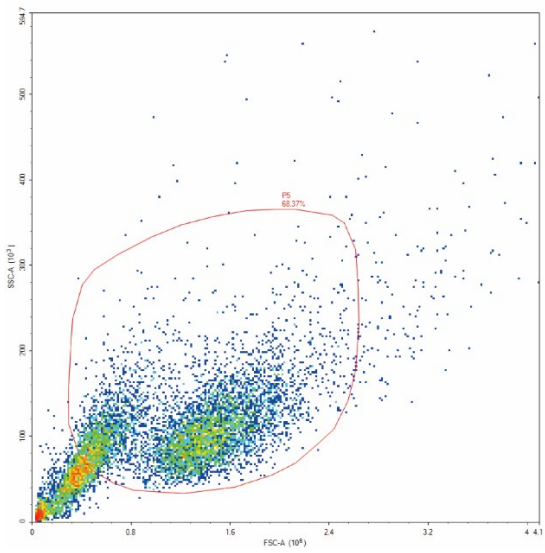

Supplementary Figure 24. Representative gating for data analyzed of M2 polarization in Supplementary Fig. 21.

Reference

1. J. W. Bortolotto, R. Margis, A. C. Ferreira, A. V. Padoin, C. C. Mottin, R. M. Guaragna, Adipose tissue distribution and quantification of PPARbeta/delta and PPARgamma1-3 mRNAs: discordant gene expression in subcutaneous, retroperitoneal and visceral adipose tissue of morbidly obese patients. *Obes. Surg.* **17**, 934-40 (2007).